Front. Chem. China 2007, 2(4): 369–377
DOI 10.1007/s11458-007-0070-0

RESEARCH ARTICLE

DU Pan, SHI Yanmao, WU Ping, ZHOU Yaoming, CAI Chenxin

Rapid functionalization of carbon nanotube and its electrocatalysis

© Higher Education Press and Springer-Verlag 2007

Abstract It was reported that carbon nanotube (CNT) was functionalized with the electroactive Nile blue (NB), which is a phenoxazine dye, by a method of adsorption to form a NB-CNT nanocomposite. The NB-CNT nanocomposite was characterized by several spectroscopic techniques, for example, Ultraviolet-visible spectroscopy (UV-VIS), Fourier transform infrared (FTIR), Raman spectroscopy and scanning electron microscopy (SEM) etc., and the results showed that NB could rapidly and effectively be adsorbed on the surface of CNT with a high stability without changing the native structure of NB and the structure properties of CNT. Moreover, it was shown that the dispersion ability of CNT in aqueous solution had a significantly improvement after CNT functionalized with NB even at a level of high concentration, for example, 5 mg of NB-CNT per 1 mL of H_2O. The NB-CNT/ glasssy carbon (GC) electrode was fabricated by modifying NB-CNT nanocomposite on the GC electrode surface and its electrochemical properties were investigated by cyclic voltammetry. The cyclic voltammetric results indicate that CNT can improve the electrochemical behavior of NB and greatly enhance its redox peak currents. While the NB-CNT/GC electrode exhibited a pair of well-defined and nearly symmetrical redox peaks with the formal potential of (-0.422 ± 0.002) V (versus SCE, 0.1 mol/L PBS, pH 7.0), which was almost independent on the scan rates, for electrochemical reaction of NB monomer; and the redox peak potential of NB polymer located at about −0.191 V. The experimental results also demonstrated that NB and CNT could synergistically catalyze the electrochemically oxidation of NADH (β-nicotinamide adenine dinucleotide, reduced form) and NB-CNT exhibited a high performance with lowing the overpotential of more than 560 mV. The NB-CNT/GC electrode could effectively sense the concentration of NADH, which was produced during the process of oxidation of substrate (e.g. ethanol) catalyzed by dehydrogenase (e.g. alcohol dehydrogenase). The presented method for functionalization of CNT had several advantages, such as rapid and facile CNT functionalization, easy electrode fabrication and high electrocatalytic activity, etc., and could be used for fabrication electrochemical biosensor on the basis of dehydrogenase.

Keywords carbon nanotube, chemically modified electrode, functionalized carbon nanotube, electrocatalysis, NADH

1 Introduction

Carbon nanotubes (CNT), which are new pseudo-one-dimensional materials, have gained considerable attention in recent years due to their unique chemo-physical properties [1–5], for example, unique metal or semicoductor conductivity, remarkable mechanical properties, good adsorption capacity and strong microwave-adsorbing properties, etc., and have been applied in many fields [4,6–16]. Unfortunately, the absence of side groups and other functionalities that can interact with the surrounding solvent sufficiently to overcome the large intertube attraction energy, responsible for their bundling, results in the material with poor solubility (or low degree of dispersion) in most solvents, especially in water. This has become a major limitation in the design of CNT-based biosensing devices. Thus, it is generally necessary and important to study the methodology of modifying the surface of CNT [17–20].

One of the common routes to modify the CNT is to chemically functionalize their sidewall by formation covalent bond [21–24], which has been used to attach the long-chain organic molecules [25], biological polypeptide chain [26,27], amino acid [28], enzyme [29], antibody [30], DNA [31], quantum dots and nanometer-sized particles [32,33] to the surface of CNT. The covalent method, however, usually includes the relatively complicated steps and requires unattractive reagents, such as oxidative treatment using concentrated HNO_3 or mixture of concentrated H_2SO_4 and HNO_3 [34,35], and/or other strong reactive reagents [36,37]. Because the oxidative

Translated from *Acta Chimica Sinica*, 2007, 65(1): 1–9 [译自: 化学学报]

DU Pan, SHI Yanmao, WU Ping, ZHOU Yaoming, CAI Chenxin (✉)
College of Chemistry and Environmental Science, Jiangsu Key Laboratory for Molecular and Medical Biotechnology, Nanjing Normal University, Nanjing 210097, China
E-mail: cxcai@njnu.edu.cn

treatment and sidewall functionalization may impair the physical and chemical properties of CNT or destroy their sp^2 structure and thus alter the inherent properties of CNT. Alternatively, physical adsorption and the polymer wrapping is an attractive and promising approach to enhance the dispersed ability and to preserve the extended π networks of CNT [38–40]. Several gas molecules (NO_2, NH_3 and O_2, etc.) [2], derivates of anthrance [38], dyes molecules [40,41] and polymer [42], such as Nafion, have been deposited on the surface of CNT using these methods. In this work, it is reported that CNT was functionalized with the electroactive Nile blue (NB) by adsorption to form NB-CNT nanocomposite. The NB-CNT was characterized by spectroscopic and electrochemical techniques. The results showed that NB can rapidly and effectively be adsorbed on the surface of CNT with a high stability without changing the native structure of NB and the structure properties of CNT. Moreover, it was shown that the dispersion ability of CNT in an aqueous solution had a significant improvement after CNT functionalized with NB. Extensive studies were made on electrochemical characteristics of this nanocomposite and electrocatalytic activities of NB-CNT towards the oxidation of NADH (*β*-nicotinamide adenine dinucleotide).

The NADH is an important small biological molecule because it is the coferment of more than 300 dehydrogenases. The determination of NADH is, however, not straightforward due to the high overpotential (usually 0.7 to 1.0 V) for the oxidation of NADH at the bare electrode, such as GC and Pt, etc.. It has been reported that some phenothiazine dye can effectively reduce the overpotential of the oxidation of NADH [43,44]. The authors have reported that the aligned CNT can reduce the overpotential significantly [45]. In this work, the authors reported that NB and CNT could synergistically catalyze the electrochemically oxidation of NADH with a high performance after CNT functionalized with NB. Comparing with the previously report [46,47], in which the redox mediator of Azure dye was covalently attached to a biocompatible polymer (chitosan) forming composite films for the amperometric determination of NADH, the present method has several advantages, such as rapid and facile CNT functionalization, easy electrode fabrication and high electrocatalytic activity, etc.

2 Experimental

2.1 Instruments and reagents

The scanning electron microscopic (SEM) images of CNT on electrode surface were obtained with a LEO 1530 VP field-emission scanning electron microscope (German). Fourier transform infrared (FTIR) spectra were recorded on KBr disk (the mass ratio of the sample to KBr is about 1 : 50) using a Nexus 670 FT-IR spectrophotometer (Nicolet Instruments, USA). For each sample, a total of 64 scans at a resolution of 4 cm^{-1} were used. The UV-Vis spectra were obtained using a Lambda 17 ultraviolet-visible spectroscopy (UV-VIS) spectrophotometer (Perkin Elmer). The micro-Raman spectrum was recorded with a Labram HR 800 UV (Jobin Yvon) Raman spectrometer at the ambient temperature using 514.5-nm excitation and a spectral slit width of 2 cm^{-1}. X-ray powder diffraction (XRD) patterns were obtained on a Shimadzu XD-3A X-ray diffractometer with Cu K_α radiation ($\lambda = 0.154\ 18$ nm), employing a scanning rate of 4°/min. The pH value of the buffer solution was determined by a PHS-4 pH-meter. The electrochemical experiments were carried out with a CHI 660B electrochemical workstation (CH Instruments) with a conventional three-electrode cell. The coiled Pt wire and the saturated calomel electrode (SCE) were used as the counter electrode and the reference electrode respectively. Buffers were purged with high-purity nitrogen for at least 30 min prior to experiments and a nitrogen environment was then kept over solutions in the cell to protect the solution from oxygen. All experiments were performed at the temperature of (22 ± 2)°C.

Prior to use, NB (85%, Aldrich) was recrystallized two times in H_2O. NADH (in the form of sodium salt, purity $>92\%$, Shanghai Lizhu Dongfeng Biotechnology, Shanghai, China), alcohol dehydrogenase (ADH, NAD^+-dependent, EC 1.1.1.1, lyophilized power, $\geqslant 0.5$ units/mg, from horse liver, Worthington), and NAD^+ (trihydrate, Sigma) were used as received. Multi-walled CNT (<10 nm in diameter, 0.5 to 500 μm in length with a specific area of more than 300 m^2/g, and purity of $>95\%$, Shenzhen Nanotech Port, Shenzhen, China) were refluxed in 3 mol/L of HNO_3 at 60°C for ca. 10 h. The sample was filtered with a minipore membrane (the pore size is 0.22 μm in diameter, Anpel), and dried under vacuum and room temperature to obtain purified CNT. The results of Raman spectroscopy (Fig. 1) and SEM images (Fig. 4(a)) indicate that the amount of amorphous carbon in CNT sample is very low and could be neglected. All other chemicals were of analytical grade. All the solutions were prepared with double-distilled water. Moreover, 0.1 mol/L phosphate buffer solutions (PBS), which were made up from Na_2HPO_4 and KH_2PO_4, were always employed as supporting electrolyte. Solutions of NADH, ADH and NAD^+ were freshly prepared using PBS immediately before each experiment.

2.2 Functionalization of CNT and preparation of the NB-CNT/ glasssy carbon (GC) electrode

In this process, 5 mg of CNT were dispersed in 1 mL of NB (5 mmol/L) aqueous solution. After being stirred for 20 min at ambient, the dispersion was filtered with a minipore size membrane, then thoroughly washed at least thrice to remove the unadsorbed or loosely adsorbed NB, and finally dried under vacuum at room temperature overnight to obtain NB-CNT composite.

Glassy carbon (GC, CH Instruments) electrode (3 mm in diameter) was polished sequentially with metallographic abrasive paper (No. 6), slurries of 0.3- and 0.05-μm alumina to mirror finish. After rinsing with double-distilled water, it was sonicated with absolute ethanol and double-distilled

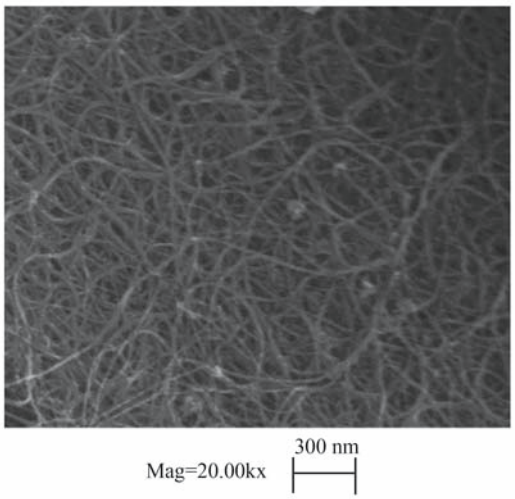

Fig. 1 A typical SEM image of NB-CNT on the surface of GC electrode

water for about 1 min, respectively. To fabricate the NB-CNT/GC electrode, 0.5 mg of NB-CNT composite was dispersed in 1 mL of H_2O giving a 0.5 mg/mL suspension. The surface of the well-polished GC was treated by casting 2 μL of NB-CNT suspension with a microsyringe and allowed the solvent (water) to evaporate at ambient temperature forming NB-CNT/GC electrode. The SEM image of NB-CNT on the surface of GC electrode is shown in Fig. 1.

The CNT/GC electrode was fabricated with the similar procedures except that CNT was dispersed in DMF (*N*,*N*-dimethylformamide) due to its poor solubility in water.

3 Results and discussion

3.1 Spectroscopic characterization of NB-CNT

When CNT was dispersed in NB solution, NB can be easily adsorbed onto the hydrophobic surface of CNT through π–π electronic interactions forming NB-CNT nanocomposites. It can be verified by UV-Vis measurements as shown in Fig. 2. The UV-Vis spectrum of NB displays an absorbance at 634 nm (Fig. 2(b)). The characteristics of spectrum of NB-SWNTs are similar to those of Nb with an absorbance at 636 nm (Fig. 2(c)), which is due to inaction between the NB and CNT. The UV-Vis spectrum of the CNT exhibits a featureless absorption. The above results suggest that NB is adsorbed on the surface of CNT. When the concentration of NB-CNT solution was increased to 1 mg/mL, a new absorbance at 595 nm is observed besides the absorbance at 636 nm (Fig. 2(d)). This new peak at 595 nm is ascribed to the absorbance of the polymer of phenothiazine dyes [40]. The polymer of NB in aqueous solution was also confirmed by UV-Vis spectra. As the concentration of NB in solution was reached to 1 mmol/L, the UV-Vis spectrum has a similar shoulder peak as that in Fig. 2(a) and (d), which indicate that NB was polymerized in aqueous solution.

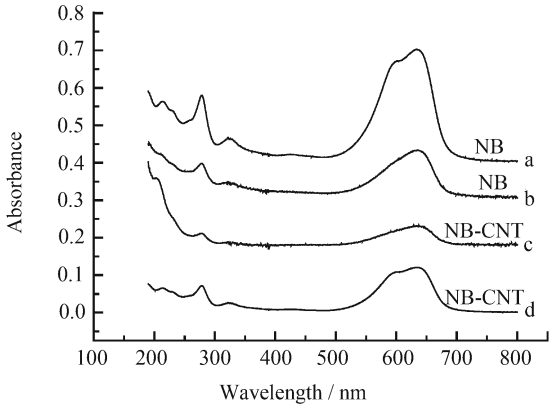

Fig. 2 UV-Vis spectra of NB in aqueous with the concentration of 1 mmol/L (a) and 0.2 mmol/L (b), and NB-CNT dispersion in water with the concentration of 0.2 mg/mL (c), 1 mg/mL (d) NB-CNT

The absorption of NB on the CNT surface is also confirmed by the IR spectra. From the IR spectra of NB-CNT(Fig. 3(a)), one can conclude the presence of the stretching vibration of aromatic ring of NB molecule (1,634 and 1,583 cm^{-1}), side-chain alkyl (1,326 cm^{-1}), tertiary amine of aromatic ring C-N (1382 cm^{-1}), C-N-C (1,260 cm^{-1}), side-chain C-N (1,168 and 1,093 cm^{-1}). These characteristic peaks are close to those in the IR spectrum of NB (Fig. 3(b)). Additionally, the peak at 1,742 cm^{-1}, which is corresponding to the carboxylic and carboxylate oxygen-contain(C=O) on the surface of the CNT [9], can also be found in the spectrum of NB-CNT.

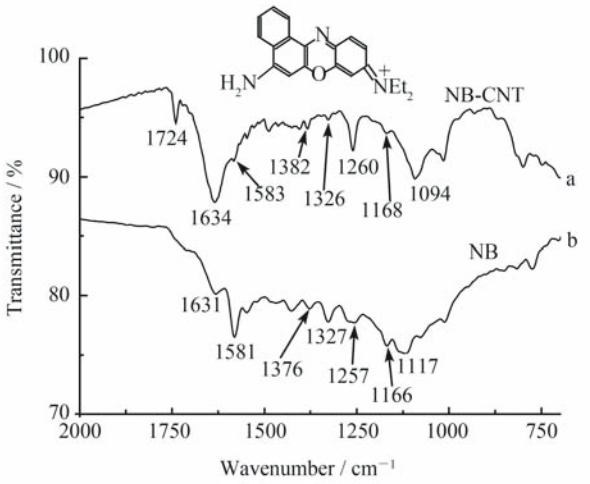

Fig. 3 IR spectra of NB-CNT (a) and free NB (b)
Note: The inset shows the structure of NB.

Figure 4(a) shows the Raman spectra of CNT. A strong peak appears at 1,587 cm^{-1}, which associates with the *G*-band, corresponding to the E_{2g} stretching mode of graphite. The appearance of peak at 1,350 cm^{-1}, the so-called *D*-line, indicates the residual ill-organized graphite (amorphous

carbon) in CNT sample [45]. The integrated relative intensities of the *D* mode versus the graphitic *G* mode shows, however, that only a minor fraction of amorphous carbon presented in the sample and the purity of the CNT sample is high. After CNT was founctionalized by NB, the peak of CNT(*G*-band) appeared at 1,590 cm^{-1} (Fig. 4(b)), it only shifted 3 cm^{-1} compared to that showing in Fig. 4(a) (1,587 cm^{-1}), indicating that the surface founctionalization does not influence the structure of CNT. The Raman spectrum of NB (Fig. 4(c)) is similar to that of NB-CNT, showing that the structure of NB itself is also not changed or destroyed.

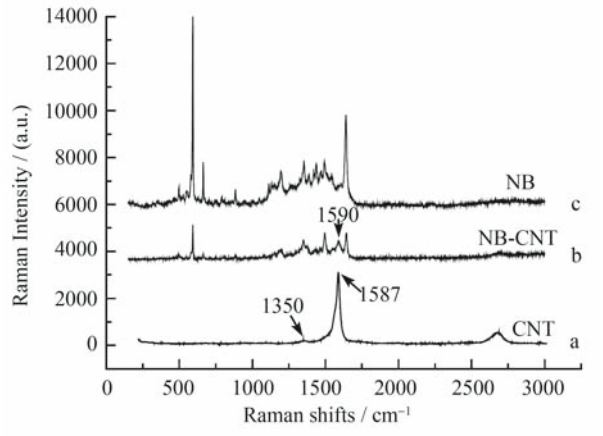

Fig. 4 Raman spectra of CNT (a), NB-CNT (b) and NB (c)

The results of XRD measurements indicate that the graphitic structure of CNT is not destroyed after they are founctionalized with NB since the characteristic diffraction peaks of C (002) and C (101), which belong to the graphitic structure of CNT, of NB-CNT (Fig. 5(b)) are almost the same as that of CNT (Fig. 5(a)).

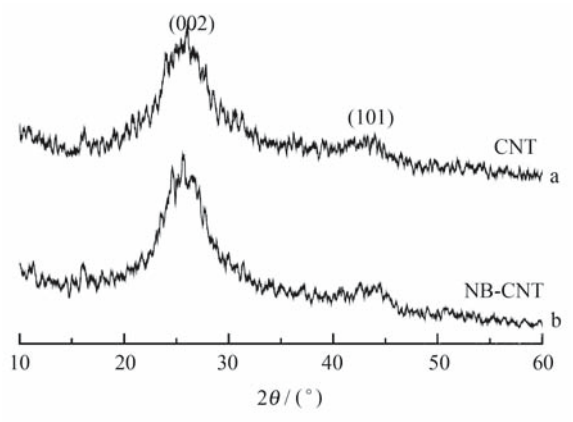

Fig. 5 XRD patterns of CNT (a) and NB-CNT (b)

All these spectroscopic results verify that the structures of CNT and NB remain unchangeable after the NB is adsorbed on the surface of CNT, indicating the interaction between NB and CNT is π-π electronic interaction.

It is found that the adsorption of NB can increase the dispersed ability of CNT in water and a black dispersion of NB-CNT can be formed and stood for a long time. The SEM image indicates that NB-CNT is untangled and uniformly covers on the surface of GC electrode (Fig. 1), while the CNT usually forms the cluster on the GC electrode surface (the SEM image of CNT on the GC electrode surface is not shown here).

3.2 Electrochemical characteristics of NB-CNT

The cyclic voltammogram of CNT/GC electrode did not show any observable redox peaks (Fig. 6(a), 0.1 mol/L PBS, pH 7.0) in the potential range of interest. It is found that the cyclic voltammetric response of CNT/GC electrode is almost unchanged upon consecutive potential cycling (for ca. 1 h), suggesting that CNT/GC electrode is stable. The cyclic voltammogram of NB-CNT/GC electrode, however, shows a pair of well-defined redox peaks (Fig. 6(b)), suggesting that the pair of redox peaks in Fig. 6(b) can be ascribed to the electrochemical reaction of NB. The cathodic (E_{pc}) and anodic (E_{pa}) potential are −454 and −387 mV, respectively, at the scan rate of 100 mV/s, and the formal potential ($E^{0'}$), which is defined as the average value of E_{pc} and E_{pa}, is −421 mV, the peak potential separation (ΔE_p) is 67 mV, which is similar to that for the NB adsorbed on the surface graphite electrode (−420 mV) [48], and is close to that for the NB adsorbed on the surface carbon fibre electrode (−410 mV) [49]. All the results suggest the formation of NB-CNT composite. This conclusion is consistent with that obtained from the spectroscopic results.

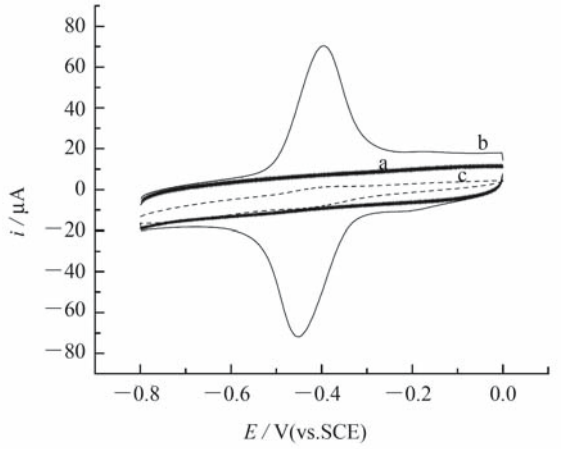

Fig. 6 Cyclic voltammograms of CNT/GC (a), NB-CNT/GC (b) and NB/GC (c) electrode in 0.1 mol/L PBS (pH 7.0) at a scan rate of 100 mV/s

The cyclic voltammogram of NB/GC electrode shows a couple of redox peaks with the $E^{0'}$ of about −410 mV (the values of E_{pc}, E_{pa}, and ΔE_p are −433, −386 and 47 mV, respectively). The value of $E^{0'}$ is similar to that of NB-CNT, the peak current, however, is very small, only 1/50 of that for NB-CNT (Fig. 6(c)). These results indicate that NB has stronger adsorption ability on CNT surface than that at GC surface.

Besides the couple of redox peaks for the electron-transfer reaction of NB monomer, a new cathodic peak with the peak potential of ca. −191 mV appears in Fig. 6(b). This new redox peaks are resulted from the NB polymer on the surface of CNT [50]. It indicates that there are some NB polymers on the surface of CNT, the conclusion of which is consistent with that obtained from the UV-Vis spectroscopic results. However, the peak current is too small to be analyzed quantitatively. Thus, only the couple of redox peaks for the electron-transfer reaction of NB monomer is discussed in the following.

The surface concentration (expressed as $A\Gamma$ in mol) of NB on the CNT can be estimated using Eq. (1)

$$A\Gamma = Q / nF \tag{1}$$

where Q is the charge consumed in coulombs, obtaining from integrating the anodic (or cathodic) peak area in cyclic voltammogram under the background correction, n the numbers of electron transfer for the reaction of NB ($n = 2$) [49], F the Faraday constant, and A the apparent area of the electrode. The results presented in Fig. 7 indicate that the value of $A\Gamma$ depends on the adsorption time (stirring time). The value of $A\Gamma$ increases with the increasing of the adsorption time, and then level off after 25 min, after that, the amount of NB on the surface of CNT tends to saturation, and the maximum value of $A\Gamma$ is about 5.1×10^{-10} mol.

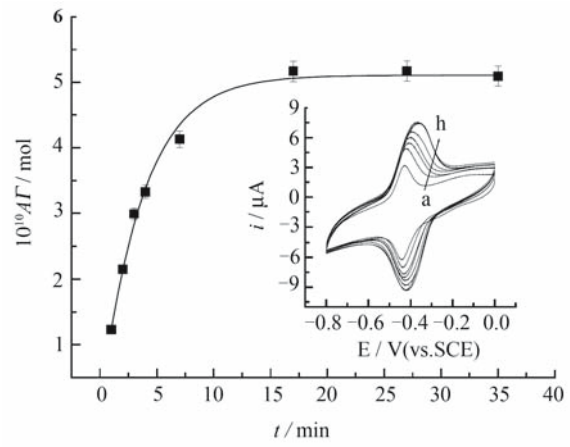

Fig. 7 Dependence of the amount of absorption ($A\Gamma$) on the time
Note: The inset shows the cyclic voltammograms of NB-CNT at a scan rate of 10 mV/s with absorption time of (from a to h) 1, 2, 3, 4, 7, 17, 27 and 35 min, respectively. The supporting electrolyte is 0.1 mol/L PBS (pH 7.0).

The redox potential and currents of NB-CNT/GC electrode are scanning rate (v) dependent. Figure 8 shows the cyclic voltammograms of the electrode at the different scanning rates. It is observed that the cathodic and anodic peak currents are almost equal at all scanning rates and increase linearly with the increasing of v (the inset A), suggesting that the overall electrochemical process is controlled by a surface reaction [51]. The values of E_{pc} and E_{pa} shift to the negative and positive directions, respectively, and ΔE_p increases with increasing scanning rates. However, $E^{0'}$ is almost independent from the scanning rates (the inset B). The peak potential (E_p) increased linearly with the scanning rates (the inset B). From the dependence of E_p and ΔE_p on the scanning rate, the charge transfer coefficient (α) and the apparent heterogeneous electron transfer rate constant (k_s) can be estimated to be 0.506 and (0.7 ± 0.3) s^{-1}, respectively, using the method developed by Laviron [52] for a surface-controlled electrochemical system (Eqs. (2)–(4)). The k_s is close to that of NB on carbon fibre (0.58 s^{-1}, pH 7.0) [49].

$$E_{pc} = E^{0'} - (RT/\alpha nF) \ln (\alpha/m) \tag{2}$$

$$E_{pc} = E^{0'} + [RT/(1-\alpha)\, nF] \ln [(1-\alpha)/m] \tag{3}$$

$$\lg k_s = \alpha \lg(1-\alpha) + (1-\alpha) \lg \alpha - \lg (RT/nFv) - \alpha (1-\alpha)\, nF\, \Delta E_p/2.3RT \tag{4}$$

where R is gas constant, T temperature, α the charge-transfer coefficient, v is scanning rate, and k_s the apparent heterogeneous electron-transfer rate constant.

$$m = (RT/F)\,(k_s/nv) \tag{5}$$

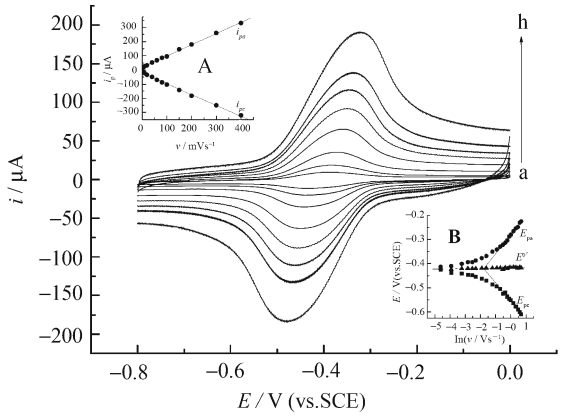

Fig. 8 Cyclic voltammograms of NB-CNT/GC electrode in 0.1 mol/L PBS (pH 7.0) at a scan rate of (a) 5, (b) 10, (c) 20, (d) 40, (e) 60, (f) 80, (g) 100 and (h) 150 mV/s
Note: The inset (A) shows the dependence of peak currents on the scan rate (v) and the inset (B) shows the dependence of peak potentials on the scan rate (ln$v$).

The stability of the voltammetric responses of the NB-CNT/GC electrode was checked with the method of continuous scanning (Fig. 9). The redox peak potential remains almost unchangeable (the inset B), and the peak currents decreases only about 4% (the inset A) after the electrode is repetitive scanned for 100 cycles, suggesting that NB is stable on the surface of CNT. The stability of the electrode is also studied by keeping it in PBS and measuring the cyclic voltammetric responses at intervals of 1–2 days. Its response decreased slowly at initial several days ($\sim$10 days), and then

the response tended to stable and still retained ca. 80% of its original response even after a storage of 20 days. Those indicate the electrode with a good stability.

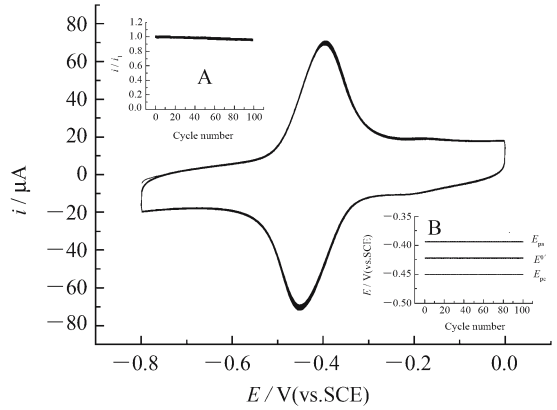

Fig. 9 Stability of the NB-CNT/GC electrode on continuously scanning 100 cycles (the main, the scan rate is 100 mV/s)
Note: The inset shows the dependence of peak current (A) and the peak potential (B) on the scan number. The fraction of peak current remained in the inset (A) was calculated by comparing the response of the electrode with that of the first cycle.

3.3 Electrocatalytic activity of NB-CNT/GC electrode to the oxidation of NADH

It has been reported that some phenothiazine dyes can effectively reduce the overpotential of the oxidation of NADH [43,44,50,53]. To examine the electrocatalytic activity of NB adsorbed on the surface of CNT to the oxidation of NADH, the cyclic voltammograms were recorded at the NB-CNT/GC electrode in the solution with the presence and absence of NADH, respectively. Figure 10(a) and (b) depict the cyclic voltammograms of NB-CNT/GC electrode in PBS (pH 7.0) in the presence (Fig. 10(a)) and absence (Fig. 10(b)) of 2 mmol/L NADH. The redox peak potential (−420 mV) of NB monomer remains almost unchangeable. Upon addition of NADH, the anodic peak currents of NB polymer increase drastically, while the cathodic peak currents decrease (compared with Fig. 10(b)). Moreover, the anodic peak potential shifts to −110 mV (Fig. 10(a)) from −191 mV, which is the anodic peak potential of NB-CNT/GC electrode in PBS without NADH presence. All those are the typical characteristics of electrocatalytic reaction, and suggest that NB being adsorbed on the surface of CNT can catalyze the electrochemical oxidation of NADH. The anodic peak potential for oxidation of NADH at NB-CNT/GC electrode is similar to that obtained at chitosan, which was covalently attached with Azure c (−80 mV) [46]. Since the anodic peak for the oxidation of NADH at bare GC electrode is at about +460 mV (Fig. 10(e)), the NB-CNT/GC electrode can lower the overpotential for more than 560 mV, suggesting that the catalytic activity of NB-CNT/GC electrode toward the oxidation of NADH is high.

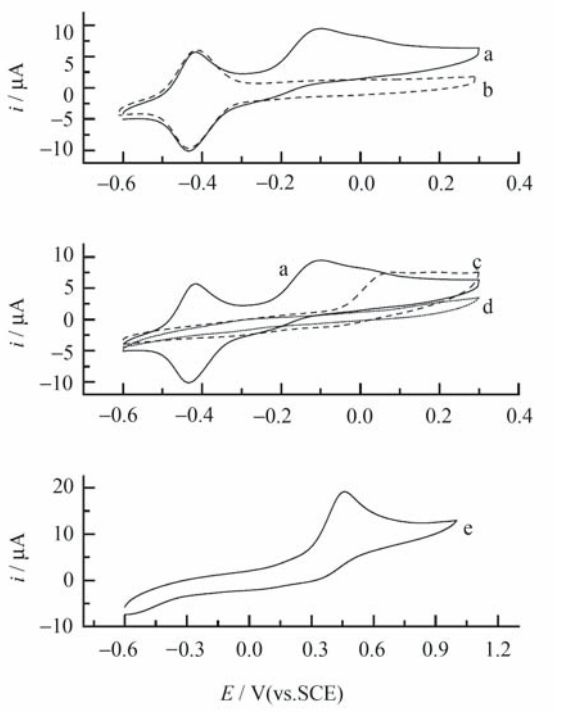

Fig. 10 Cyclic voltammograms of NB-CNT/GC (a, b), CNT/GC (c), NB/GC (d) and bare GC (e) electrode in 0.1 mol/L PBS (pH 7.0) in the presence (a, c, d, e) and absence (b) of 2 mmol/L NADH at a scan rate of 10 mV/s

To further clarify the function of CNT in NB-CNT composite in the process of catalytic oxidation of NADH, the cyclic voltammograms of the oxidation of NADH at CNT/GC and NB/GC electrode were recorded respectively. The results are presented in the Fig; 10(a), (c) and (d). The anodic peak for the oxidation of NADH at CNT/GC electrode is at 70 mV, thus, the CNT/GC electrode can reduce the overpotential of ca. 390 mV. Furthermore, the anodic peak current for the oxidation of NADH at the NB-CNT/GC electrode is significantly higher than that at the CNT/GC electrode. The catalytic activity of the NB/GC electrode to the oxidation of NADH is not very obvious, and it is hard to perform the quantitative analysis. All the above results demonstrate that NB and CNT could synergistically catalyze the electrochemically oxidation of NADH. This may be ascribed to NB-CNT nanocomposite and higher conductivity of CNT.

The stability of the NB-CNT/GC electrode catalyzing the oxidation of NADH was checked with the method of continuous scanning. The catalytic currents decreased rapidly at the initial several cycles (the second only remained 67% of the first), after that, the currents decrease became slowly. After five cycles, the catalytic currents increased slowly; after ten cycles, the catalytic currents tended to relatively stable value. The catalytic peak currents could remain about 67% of that for the first cycle after the electrode was repetitive scanned 30 cycles (Fig. 11). The response kept about 83% of its original response after the electrode was stored in PBS

for one week, suggesting that electrocatalytic activity of NB-CNT/GC electrode is stable.

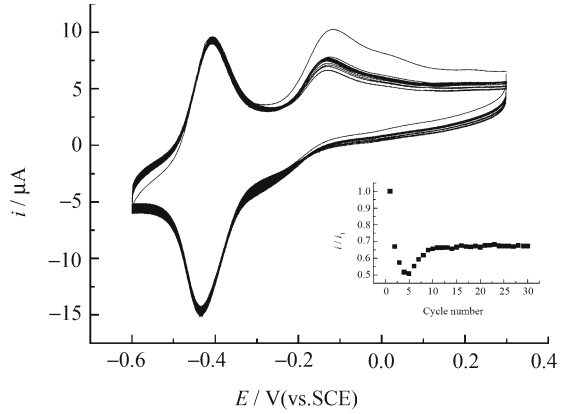

Fig. 11 Stability of the NB-CNT/GC electrode in PBS (0.1 mol/L, pH 7.0) containing 2 mmol/L NADH on the continuously scanning (the main, the scan rate is 10 mV/s)
Note: The inset shows the dependence of the catalytic current on the scan number. The fraction of catalytic current remaining was calculated by comparing the response of the electrode with that of the first cycle.

3.4 Electrochemical oxidation of ethanol on NB-CNT/GC electrode

To study the potential application of NB-CNT in the fabrication of the dehydrogenase-based biosensors, the ADH was selected as a model. The sensing characteristics of the NB-CNT/GC electrode to the ethanol were recorded as shown in Fig. 12, which was carried out in the solution with and without presence of ethanol, respectively. No electrochemical response is observed for the NB-CNT/GC electrode in 0.1 M PBS (pH 7.0) in the presence of 2.5 mg/mL ADH and 3 mmol/L NAD^+ at a scan rate of 5 mV/s in the potential range of interest (Fig. 12(a)). Upon the addition of 10 mmol/L of ethanol, the cyclic voltammogram was characterized by a large anodic peak and the peak potential was at ca. 5 mV (Fig. 12(b)). The response current is resulted from the electrocatalytic oxidation of NADH, which is produced in the enzymatic reaction at the NB-CNT/GC electrode (Compared with Fig. 10(a), the catalytic anodic peak potential of NADH shift 115 mV, which may result from the composition of system). The inset of Fig. 12 shows the reaction process. These results indicate that the NB-CNT/GC electrode has bioelectrocatalytic activities to catalyze the oxidation of ethanol and can be used as a biosensor to sense the substrate.

4 Conclusion

The CNT was rapidly and effectively functionalized with NB with a method of adsorption to form an NB-CNT nanocomposite without changing the native structure of NB and the structure properties of CNT. Moreover, the dispersion ability of CNT in aqueous solution had a significantly improvement after CNT functionalized with NB. The voltammetric results demonstrated that NB and CNT could synergistically catalyze the electrochemically oxidation of NADH with lowing the overpotential for more than 560 mV. The NB-CNT/GC electrode could effectively sense the concentration of NADH, which was produced during the process of oxidation of substrate (for example ethanol) catalyzed by dehydrogenase (for example alcohol dehydrogenase). The presented method for functionalization of CNT has several advantages, such as rapid and facile CNT functionalization, easy electrode fabrication and high electrocatalytic activity, etc., and could be used for fabrication electrochemical biosensor on the basis of dehydrogenase.

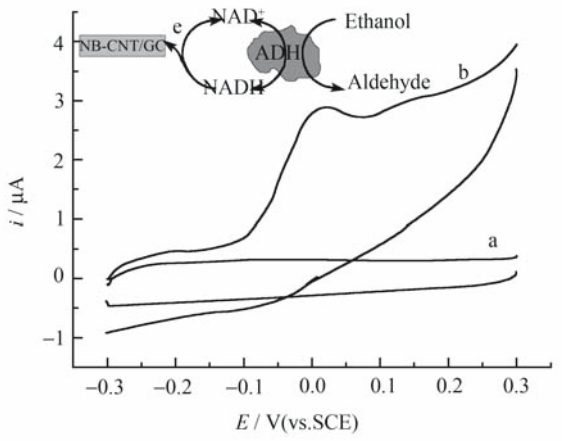

Fig. 12 Cyclic voltammograms of NB-CNT/GC electrode in 0.1 mol/L PBS (pH 7.0) containing 2.5 mg/mL ADH and 3 mmol/L NAD^+ in absence (a) and presence (b) of 10 mmol/L ethanol (scan rate: 5 mV/s)
Note: The inset shows the schematic diagram of oxidation of ethanol catalyzed by alcohol dehydrogenase.

Acknowledgements This work was supported by the National Natural Science Foundation of China (Grant No. 20373027, 20673057), the Program for New Century Excellent Talents in University (No. NCET) of MOE, the Natural Science Foundation of Jiangsu Province (No. BK2005138), and the Foundation of the Jiangsu Key Laboratory for Molecular and Medical Biotechnology, China (No. MMBKF05001).

References

1. Ajayan P M. Nanotubes from carbon. Chem Rev, 1999, 99: 1, 787–1,799
2. Dai H. Carbon nanotubes: Opportunities and challenges. Surf Sci, 2002, 500: 218–241
3. Belin T, Epron F. Characterization methods of carbon nanotubes: A review. Materials Science & Engineering B, 2005, 119: 105–118
4. Gooding J J. Nanostructuring electrodes with carbon nanotubes: A review on electrochemistry and applications for sensing. Electrochim. Acta, 2005, 50: 3,049−3,060

5. Wang J. Carbon-nanotube based electrochemical biosensors: A review. Electroanalysis, 2005, 17: 7–14
6. Cai Chenxin, Chen Jing, Bao Jianchun, Lu Tianhong. Applications of carbon nanotubes in analytical chemistry. Chin J Anal Chem, 2004, 32: 381–387 (in Chinese)
7. Wang Z, Luo G A. The progress of carbon nanotube in analytical chemistry. Chin J Anal Chem, 2003, 31: 1,004–1,009 (in Chinese)
8. Cai Chenxin, Chen Jing. Direct electrochemistry of horseradish peroxidase at a carbon nanotube electrode. Acta Chim Sinica, 2004, 62: 335–340 (in Chinese)
9. Cai Chenxin, Chen Jing, Lu Tianhong. Direct electron-transferof glucose oxidase at the carbon nanotubes modified electrode. Sci in China (Ser B), 2003, 33: 511–518 (in Chinese)
10. Chen J, Cai C X. Direct electrochemical oxidation of NADPH at a low potential on the carbon nanotube modified glassy carbon electrode. Chin J Chem, 2004, 22: 167–171
11. Wang M K, Shen Y, Liu Y, Wang T, Zhao F, Liu B F, Dong S J. Direct electrochemistry of microperoxidase 11 using carbon nanotube modified electrodes. J Electroanal Chem, 2005, 578: 121–127
12. Xu J J, Wang G, Zhang Q, Zhou D M, Chen H Y. Interfacing cytochrome c to Au electrodes with humic acid film. Electrochem Commun, 2004, 6: 278−283
13. Zhao G C, Yin Z Z, Zhang L, Wei X W. Direct electrochemistry of cytochrome c on a multi-walled carbon nanotubes modified electrode and its electrocatalytic activity for the reduction of H_2O_2. Electrochem Commun, 2005, 7: 256–260
14. Wang J X, Li M X, Shi Z J, Li N Q, Gu Z N. Direct electrochemistry of cytochrome c at a glassy carbon electrode modified with single-wall carbon nanotubes. Anal Chem, 2002, 74: 1,993–1,997
15. Cai C X, Chen J. Direct electron transfer and bioelectrocatalysis of hemoglobin at a carbon nanotube electrode. Anal Biochem, 2004, 325: 285–292
16. Xu J X, Zhu J J, Wu Q, Hu Z, Chen H Y. Direct electron transfer between glucose oxidase and multi-walled carbon nanotubes. Chin J Chem, 2003, 21: 1,088–1,091
17. Ouyang M, Huang J L, Lieber C M. Fundamental electronic properties and applications of single-walled carbon nanotubes. Acc Chem Res, 2002, 35: 1,018–1,025
18. Dai H J. Carbon nanotubes: Synthesis, integration, and properties. Acc Chem Res, 2002, 35: 1,035–1,044
19. Sun Y P, Fu K, Huang W. Functionalized carbon nanotubes: Properties and applications. Acc Chem Res, 2002, 35: 1, 096–1,104
20. Niyogi R, Hamon M A, Haddon R C. Chemistry of single-walled carbon nanotubes. Acc Chem Res, 2002, 35, 1,105–1,113
21. Dyke C A, Tour J M. Decomposing complex cooperative ligand binding into simple components: Connections between microscopic and macroscopic models. J Phys Chem B, 2004, 108: 11,151–11,169
22. Hong C Y, You Y Z, Pan C Y. Synthesis of water-soluble multiwalled carbon nanotubes with grafted temperature-responsive shells by surface RAFT solymerization. Chem Mater, 2005, 17: 2,247–2,254
23. Gómez F J, Chen R J, Wang D, Waymouth R M, Dai H. Ring opening metathesis polymerization on non-covalently functionalized single-walled carbon nanotubes electronic supplementary information (ESI) available: Full experimental details for compounds 2–4, nanotube preparation and microscopy analysis. Chem Commun, 2003, 190–191
24. Holzinger M, Abraham J, Whelan P, Graupner R, Ley L, Hennrich F, Kappes M, Hirsch A. Functionalization of single-walled carbon nanotubes with (R-) oxycarbonyl nitrenes. J Am Chem Soc, 2003, 125: 8,566–8,580
25. Chen J, Hamon M A, Hu H, Chen Y, Rao A M, Eklund P C, Haddon R C. Solution properties of single-walled carbon nanotubes, Science, 1998, 282: 95–98
26. Pantarotto D, Partidos C D, Graff R, Hoebeke J, Briand J P, Prato M, Bianco A. Synthesis, structural characterization, and immunological properties of carbon nanotubes functionalized with peptides. J Am Chem Soc, 2003, 125: 6,160–6,164
27. Dieckmann G R, Dalton A B, Johnson P A, Razal J, Chen J, Giordano G M, Muñoz E, Musselman I H, Baughman R H, Draper R. K. Controlled assembly of carbon nanotubes by designed amphiphilic peptide helices. J Am Chem Soc, 2003, 125: 1,770–1,777
28. Georgalilas Y, Tagmatarchis N, Pantarotto D, Bianco A, Briand J P, Prato M. Amino acid functionalisation of water soluble carbon nanotubes. Chem Commun, 2002, 3,050–3,051
29. Azamian B R, Davis J J. Bioelectrochemical single-walled carbon nanotubes. J Am Chem Soc, 2002, 124: 12,664–12,665
30. Shim M, Kam N W, Dai H J. Functionalization of carbon nanotubes for biocompatibility and biomolecular recognition. Nano Lett, 2002, 2: 285–288
31. Baker S E, Cai W. Covalently bonded adducts of deoxyribonucleic acid (DNA) oligonucleotides with single-wall carbon nanotubes: Synthesis and hybridization. Nano Lett, 2002, 2: 1,413–1,417
32. Haremza J M, Kahn M A. Attachment of single CdSe nanocrystals to individual single-walled carbon nanotubes. Nano Lett, 2002, 2: 1,253–1,258
33. Whitby R L D, Hsu W K, Collison D. Multiwalled carbon nanotubes coated with tungsten disulfide. Chem Meter, 2002, 14: 2,209–2,217
34. Stephenson J J, Hudson J L, Azad S, Tour J M. Individualized single walled carbon nanotubes from bulk material using 96% sulfuric acid as solvent. Chem Mater, 2006, 18: 374–377
35. Wang Y, Iqbal Z, Mitra S. Rapidly functionalized, water-dispersed carbon nanotubes at high concentration. J Am Chem Soc, 2006, 128: 95–99
36. Mickelson E T. Fluorination of single-wall carbon nanotubes. Chem Phys Chem, 1998, 296: 188−194
37. Banerjee S, Wong S S. Rational sidewall functionalization and purification of single-walled carbon nanotubes by solution-phase ozonolysis. J Phys Chem B, 2002, 106: 12,144–12,151
38. Chen R J, Zhang Y, Wang D, Dai H J. Noncovalent sidewall functionalization of single-walled carbon nanotubes for protein immobilization. J Am Chem Soc, 2001, 123: 3,838–3,839
39. Star A, Stoddart J F, Steuerman D, Diehl M, Boukai A, Wong E W, Yang X, Chung S W, Choi H, Heath J R. Preparation and properties of polymer-wrapped single-walled carbon nanotubes. Angew Chem Int Ed, 2001, 40: 1,721–1,725
40. Yan Y M, Zhang M N, Gong K P, Su L, Guo Z X, Mao L Q. Adsorption of methylene blue dye onto carbon nanotubes: A route to an electrochemically functional nanostructure and its layer-by-layer assembled nanocomposite. Chem Mater, 2005, 17: 3,457–3,463
41. Li Q W, Zhang J, Yan H, He M S, Liu Z F. Thionine-mediated chemistry of carbon nanotubes. Carbon, 2004, 42: 287–291
42. Wang J, Musameh M, Lin Y. Solubilization of carbon nanotubes by nafion toward the preparation of amperometric biosensors. J Am Chem Soc, 2003, 125: 2,408–2,409
43. Gorton L. Chemically modified electrodes for the electrocatalytic oxidation of nicotinamide coenzymes. J Chem Soc Faraday Trans I, 1986, 82: 1,245–1,258
44. Persson B. A chemically modified graphite electrode for electrocatalytic oxidation of reduced nicotinamide adenine dinucleotide based on a phenothiazine derivative, 3-b-naphthoyl-toluidine blue. J Electroanal Chem, 1990, 287: 61–80

45. Chen J, Bao J C, Cai C X, Lu T H. Electrocatalytic oxidation of NADH at an ordered carbon nanotubes modified glassy carbon electrode. Anal Chim Acta, 2004, 516: 29–34
46. Zhang M G, Gorski W. Electrochemical sensing based on redox mediation at carbon nanotubes. Anal Chem, 2005, 77: 3,960–3,965
47. Zhang M G, Gorski W. Electrochemical sensing platform based on the carbon nanotubes/redox mediators-biopolymer system. J Am Chem Soc, 2005, 127: 2,058–2,059
48. Persson B, Gorton L. A comparative study of some 3,7-diaminophenoxazine derivatives and related compounds for electrocatalytic oxidation of NADH. J Electroanal Chem, 1990, 292: 115–138
49. Ju H X, Dong L, Chen H Y. The study on the electrochemical behaviour of nile blue A modified carbon fiber microcylinder electrode. Chem J Chin Univ, 1995, 16: 1,200–1,203 (in Chinese)
50. Cai C X, Xue K H. Electrocatalytic oxidation of NADH at glassy carbon electrodes modified with an electropolymerized film of nile blue. Chin J Chem, 2000, 18: 182–187
51. Bard A J, Faulkner L R. Electrochemical Methods, Fundamental and Applications. 2nd ed, New York: John Wiley & Sons Inc, 2001, 594
52. Laviron E. General expression of the linear potential sweep voltammogram in the case of diffusionless electrochemical systems. J Electroanal Chem, 1979, 101: 19–28
53. Cai C X, Xue K H. Electrocatalysis of NADH oxidation with electropolymerized films of azure I. J Electroanal Chem, 1997, 427: 147–153